Available online at www.sciencedirect.com
SCIENCE DIRECT®
Journal of Sound and Vibration 281 (2005) 1163–1174
JOURNAL OF SOUND AND VIBRATION
www.elsevier.com/locate/jsvi

Short Communication

Optimization of a rotating flexible arm with ACLD treatment

D.T.W. Yau, E.H.K. Fung*

Department of Mechanical Engineering, The Hong Kong Polytechnic University, Hung Hom, Kowloon, Hong Kong, People's Republic of China

Received 8 December 2003; accepted 25 March 2004

1. Introduction

The concept of the active constrained layer damping (ACLD) treatment is typically a three-layer composite consisting of a passive viscoelastic damping layer sandwiched between an active piezoelectric actuator layer (piezo-constraining layer) and a piezoelectric sensor layer. The treatment is bonded to the beam structure and has been demonstrated as an effective means for vibration suppression and control [1,2]. To enhance the effectiveness of the ACLD treatments, many researchers investigated the optimal design and control problem of the system [3–9]. The objective of the optimal design is usually to maximize the modal damping ratios, modal strain energies or energy dissipation coefficients and/or minimize the weight of the damping treatment by selecting the optimal variables such as the placement and/or sizing of the ACLD treatment, thickness and shear modulus of the viscoelastic material (VEM) cores, piezo-electric sensor/actuator parameters, control gains, etc. In the optimal control problem, the objective is usually to select the optimal control gains to minimize a quadratic performance index which is equal to a weighted sum of the vibrational and control energies. The control performance index is expressed in terms of the initial states of the system and the optimal control problem is posed to solve a min–max problem [3]. This control objective can also be used to determine the optimal design variables such as placement and sizing of the piezoelectric actuator [10,11].

*Corresponding author. Tel.: +852-2766-6647; fax: +852-2365-4703.
E-mail address: mmhkfung@polyu.edu.hk (E.H.K. Fung).

0022-460X/$ - see front matter
doi:10.1016/j.jsv.2004.03.054

The vibration characteristics of a rotating flexible beam with ACLD treatment have been studied in Ref. [12]. This paper extends the work to study the optimal design and control of the same system. The flexible arm, which is fully covered with ACLD treatment, is rotating in a horizontal plane in which the gravitational effect and rotary inertia are neglected. The VEM behavior is described using the complex shear modulus approach [13]. A PD controller is used in this investigation. The finite element equations of motion of the system are presented. The optimal design variables such as the PZT actuator thickness, viscoelastic layer thickness and storage shear modulus are determined by maximizing the sum of the first three open-loop modal damping ratios divided by the weight of the damping treatment. The optimal control gains are determined by solving a min–max control optimization problem. Frequency response and impulse response of the beam tip under different value of the control gains are also presented. The results of this study will be useful in the optimal design and control of rotating adaptive and smart structures such as rotorcraft blades or robotic arms.

2. Finite element equations of motion

A finite element of a clamped-free flexible arm with fully covered ACLD treatment is shown in Fig. 1. The arm is of length L and is rotating in a horizontal plane at constant angular velocity $\dot{\theta}$ about the clamped axis. The thickness and density of the kth layer are denoted by h_k and ρ_k respectively. The axial deformation u_k and the transverse displacement w (chordwise bending) of all three layers are in the plane of rotation. The subscripts 1, 2 and 3 denote the piezo-actuator layer, the viscoelastic layer and the piezo-sensor/beam, respectively. The detailed derivation of the finite element equations of motion has been presented in Ref. [12]. The linearized equation of motion at the element level can be written as

$$\mathbf{M}_{qqi}\ddot{\mathbf{q}}_i + 2\dot{\theta}\mathbf{G}_i\dot{q}_i + \mathbf{K}_{qqi}\mathbf{q}_i = \mathbf{F}_{ci} + \mathbf{F}_{di}, \tag{1}$$

where $\mathbf{q}_i$ is the nodal deflection vector bounded between nodes j and k of the ith element, which is given by $\mathbf{q}_i = \{u_{1j}u_{3j}w_jw_{jx}u_{1k}u_{3k}w_kw_{kx}\}^{\mathrm{T}}$ where the subscript x denotes differentiation with respect to the elemental coordinate x. $\mathbf{M}_{qqi}$ is the real symmetric positive definite generalized mass matrix. $\mathbf{G}_i$ is the real skew symmetric gyroscopic matrix. $\mathbf{K}_{qqi}$ is the generalized stiffness matrix which is complex due to the complex shear modulus G_2 of the VEM such that $G_2 = G_2'(1 + \eta i)$, where G_2' is the storage modulus and η is the loss factor at a nominal operating temperature and frequency. The matrices $\mathbf{F}_{ci}$ and $\mathbf{F}_{di}$ represent the control force vector and the external load, respectively. All the above matrices and vectors are given in Ref. [12]. With PD controller applied to the piezo-sensor, the control force vector $\mathbf{F}_{ci}$ and the output equation $\mathbf{y}_i$ can be written as

$$\mathbf{F}_{ci} = K_p \cdot \mathbf{B}_{0i}\mathbf{q}_i + K_d \cdot \mathbf{B}_{0i}\dot{\mathbf{q}}_i, \tag{2}$$

$$\mathbf{y}_i = \mathbf{C}_i\mathbf{x}_i, \tag{3}$$

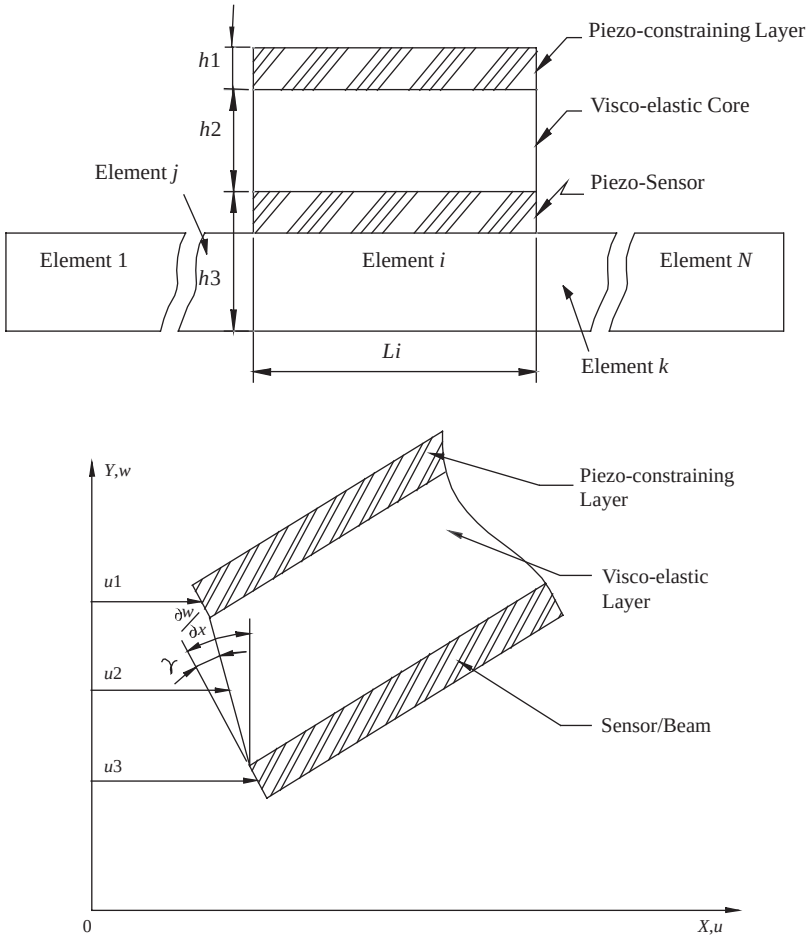

Fig. 1. A finite element of the rotating flexible arm with fully covered ACLD treatment.

where

$$\mathbf{x}_i = [\mathbf{q}_i^{\mathrm{T}} \;\; \dot{\mathbf{q}}_i^{\mathrm{T}}]^{\mathrm{T}},$$

$$\mathbf{B}_{0i} = \begin{bmatrix} -1 & 0 & 0 & 0 & 1 & 0 & 0 & 0 \\ 0 & 0 & 0 & -1 & 0 & 0 & 0 & 1 \end{bmatrix}^{\mathrm{T}} \cdot \begin{bmatrix} 0 & 0 & 0 & -g/2 & 0 & 0 & 0 & g/2 \\ 0 & 0 & 0 & -gh/2 & 0 & 0 & 0 & gh/2 \end{bmatrix}, \tag{4a–c}$$

$$\mathbf{C}_i = \begin{bmatrix} 0 & 0 & 0 & -1 & 0 & 0 & 0 & 1 & \mathbf{0}_{1\times 8} \end{bmatrix},$$

$\mathbf{B}_{0i}$ is the voltage factored out electrical loads matrix; h and g are parameters defined in Ref. [12]; K_p and K_d are the proportional and derivative control gains, respectively.

The global equation is obtained using the standard finite element assembling procedure of the elemental coefficient matrices. Combining and assembling the elemental coefficient

matrices of Eqs. (1), (2) and (3) lead to the following global dynamical equations of the system in state space form:

$$\begin{aligned} \dot{\mathbf{x}} &= \mathbf{A}\mathbf{x} + \mathbf{B}\mathbf{u} + \mathbf{p}, \\ \mathbf{y} &= \mathbf{C}\mathbf{x} \quad \text{and} \quad \mathbf{u} = \mathbf{D}\mathbf{x}, \end{aligned} \tag{5}$$

where

$$\mathbf{x} = [\mathbf{q}^{\mathrm{T}} \;\; \dot{\mathbf{q}}^{\mathrm{T}}]^{\mathrm{T}},$$

$$\mathbf{A} = \begin{bmatrix} \mathbf{0} & \mathbf{I} \\ -\mathbf{M}_{qq}^{-1}\mathbf{K}_{qq} & -2\dot{\theta}\,\mathbf{M}_{qq}^{-1}\mathbf{G} \end{bmatrix}, \quad \mathbf{B} = \begin{bmatrix} \mathbf{0} \\ \mathbf{M}_{qq}^{-1}\mathbf{B}_0 \end{bmatrix}, \tag{6a–e}$$

$$\mathbf{p} = \begin{bmatrix} \mathbf{0} \\ \mathbf{M}_{qq}^{-1}\mathbf{F}_d \end{bmatrix}, \quad \mathbf{D} = \begin{bmatrix} K_p\mathbf{I} & K_d\mathbf{I} \end{bmatrix}$$

x, **A** and **B** denote the vector of state variables, the open-loop system matrix and the feedback control matrix respectively. **y**, **C** and **D** denote the output vector, output measurement matrix and control gain matrix respectively. **u** is the control input and **p** is the external load state vector. The matrices in Eqs. (5) and (6) without the subscript i denote the global forms of the corresponding elemental coefficient matrices. The boundary conditions at the global origin (the clamped end) are zero for both the axial and transverse displacement of the layers.

3. Optimal design and control

The open-loop system vibration characteristic is optimized by finding the optimal design variables such as the PZT actuator thickness h_1, viscoelastic layer thickness h_2 and storage shear modulus $G_2'$of the VEM. The damping ratios ξ_i of the open-loop system can be found by solving the eigenvalues of the open-loop system matrix **A**. In this paper, the design objective function J_d is defined as the sum of the first three open-loop modal damping ratios divided by the weight of the damping treatment. The optimal design problem is formulated as searching h_1, h_2, and G_2' to maximize the design objective function

$$J_d = \frac{\xi_1 + \xi_2 + \xi_3}{\rho_1 h_1 + \rho_2 h_2 + \rho_3 h_3} \tag{7}$$

such that properties of base beam and constraining layer are known, loss factor η of VEM and the angular velocity $\dot{\theta}$ of the beam are set at a desired value.

A genetic algorithm, differential evolution (DE), combined with a gradient-based algorithm, sequential quadratic programming (SQP), is used to determine the optimum design variables [8]. The DE algorithm is a population based stochastic function minimizer developed by Price and Storn [http://www.icsi.berkeley.edu/~storn/code.html]. Its advantage is that it can avoid local minima while its disadvantage is the slow convergence as compared to a gradient-based algorithm such as SQP. To improve the speed and precision, the maximum number of iterations (generations) of the DE algorithm is initially set. DE is then used to find an initial value that is

very close to the optimal global value. Finally, the gradient-based algorithm SQP is used to converge this value to the global minimum effectively.

The closed-loop equations of the system can be written as

$$\dot{\mathbf{x}} = (\mathbf{A} + \mathbf{BD})\mathbf{x} + \mathbf{p}, \quad \mathbf{x}(0) = \mathbf{x}_0,$$
$$\mathbf{y} = \mathbf{C}\mathbf{x} \quad \text{and} \quad \mathbf{u} = \mathbf{D}\mathbf{x}. \tag{8}$$

The optimal control gains K_p and K_d are determined by minimizing the following quadratic performance index

$$J_c = \int_0^\infty (\mathbf{y}^{\mathrm{T}}\mathbf{Q}\mathbf{y} + \mathbf{u}^{\mathrm{T}}\mathbf{R}\mathbf{u})\mathrm{d}t. \tag{9}$$

Provided that system (8) satisfies the standard conditions of stabilizability and detectability, the performance index J_c can be expressed as a quadratic form in the initial conditions [14]

$$J_c = \mathbf{x}_0^{\mathrm{T}}\mathbf{P}(0)\mathbf{x}_0, \tag{10}$$

where $\mathbf{P}$ is the symmetric positive definite matrix obtained by solving the following Lyapunov matrix equation:

$$(\mathbf{A} + \mathbf{BD})^{\mathrm{T}}\mathbf{P} + \mathbf{P}(\mathbf{A} + \mathbf{BD}) + \mathbf{C}^{\mathrm{T}}\mathbf{Q}\mathbf{C} + \mathbf{D}^{\mathrm{T}}\mathbf{R}\mathbf{D} = \mathbf{0}. \tag{11}$$

In order to make the performance index J_c independent of the initial states it is normalized with respect to the initial state $\mathbf{x}_0$. The worst case performance is then employed. The performance index can be written as

$$M_c = \max_{\mathbf{x}_0} \frac{J_c}{\mathbf{x}_0^{\mathrm{T}}\mathbf{x}_0}. \tag{12}$$

It is shown by Baz and Ro [3] that M_c is equal to the maximum eigenvalue $\lambda_{\max}$ of the $\mathbf{P}$ matrix. The optimal control problem is therefore posed to determine the controller gains K_p and K_d for the following min–max optimization:

$$\min_{K_p,K_d} \max_i \lambda_i(\mathbf{P}) \tag{13}$$

such that Eq. (11) is satisfied.

4. Optimization results

The design optimization of the open-loop system is performed using the system parameters and material properties in Ref. [12]. The arm is divided into five equal finite elements along its length. The constraint conditions for the three design variables, namely the PZT actuator thickness h_1, viscoelastic layer thickness h_2 and storage modulus G_2' of the VEM are

$$0.5\,\mathrm{mm} \leqslant h_1 \leqslant 4\,\mathrm{mm},$$
$$0.01\,\mathrm{mm} \leqslant h_2 \leqslant 20\,\mathrm{mm},$$
$$0.01\,\mathrm{MPa} \leqslant G_2' \leqslant 10\,\mathrm{MPa}.$$

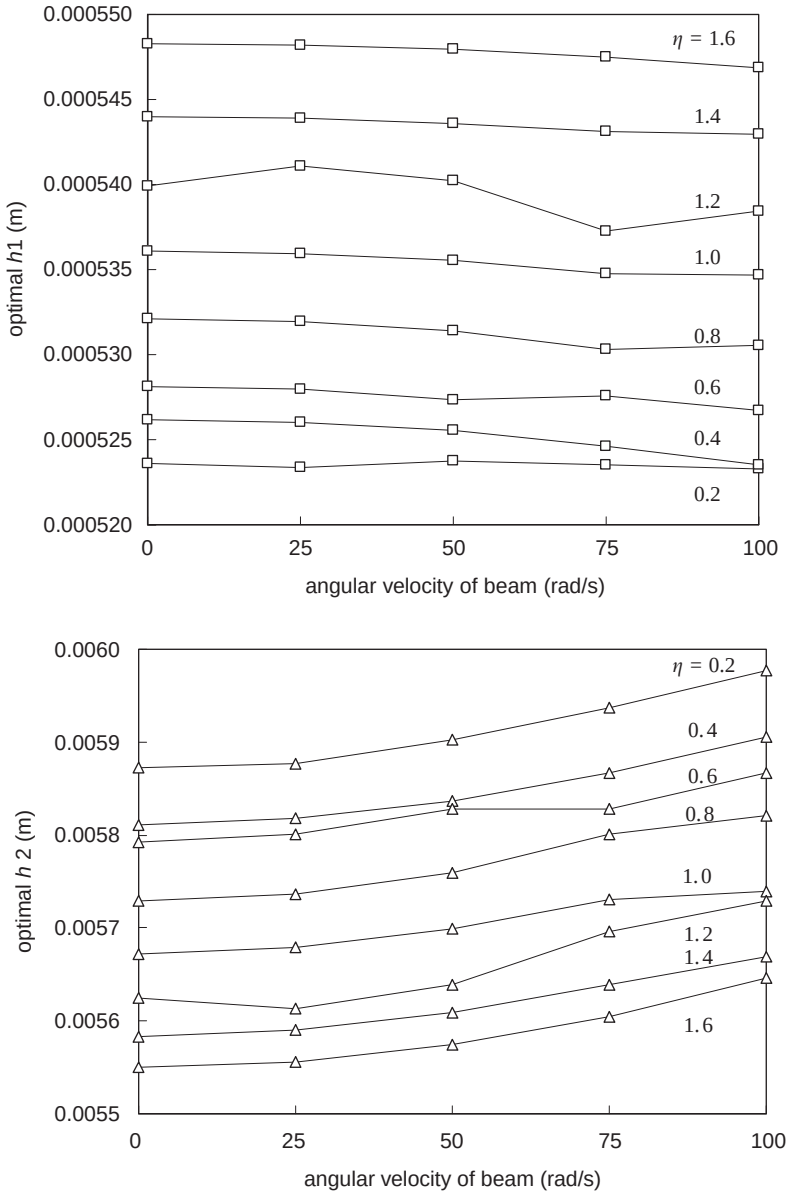

Fig. 2. Optimal h_1 and h_2 versus angular velocity of beam $\dot{\theta}$ for different VEM loss factor η.

The optimal h_1 and h_2 values versus angular velocity of beam $\dot{\theta}$ for different VEM loss factor η are plotted in Fig. 2. It can be seen that the optimal h_1 increases with increasing η while the optimal h_2 decreases with increasing η. It is also shown that, in general, the optimal h_1 decreases slightly with increasing $\dot{\theta}$ while the optimal h_2 increases as $\dot{\theta}$ increases. The optimal G_2' for the present system is 7.4704 MPa and is found to remain unchanged for different η and $\dot{\theta}$.

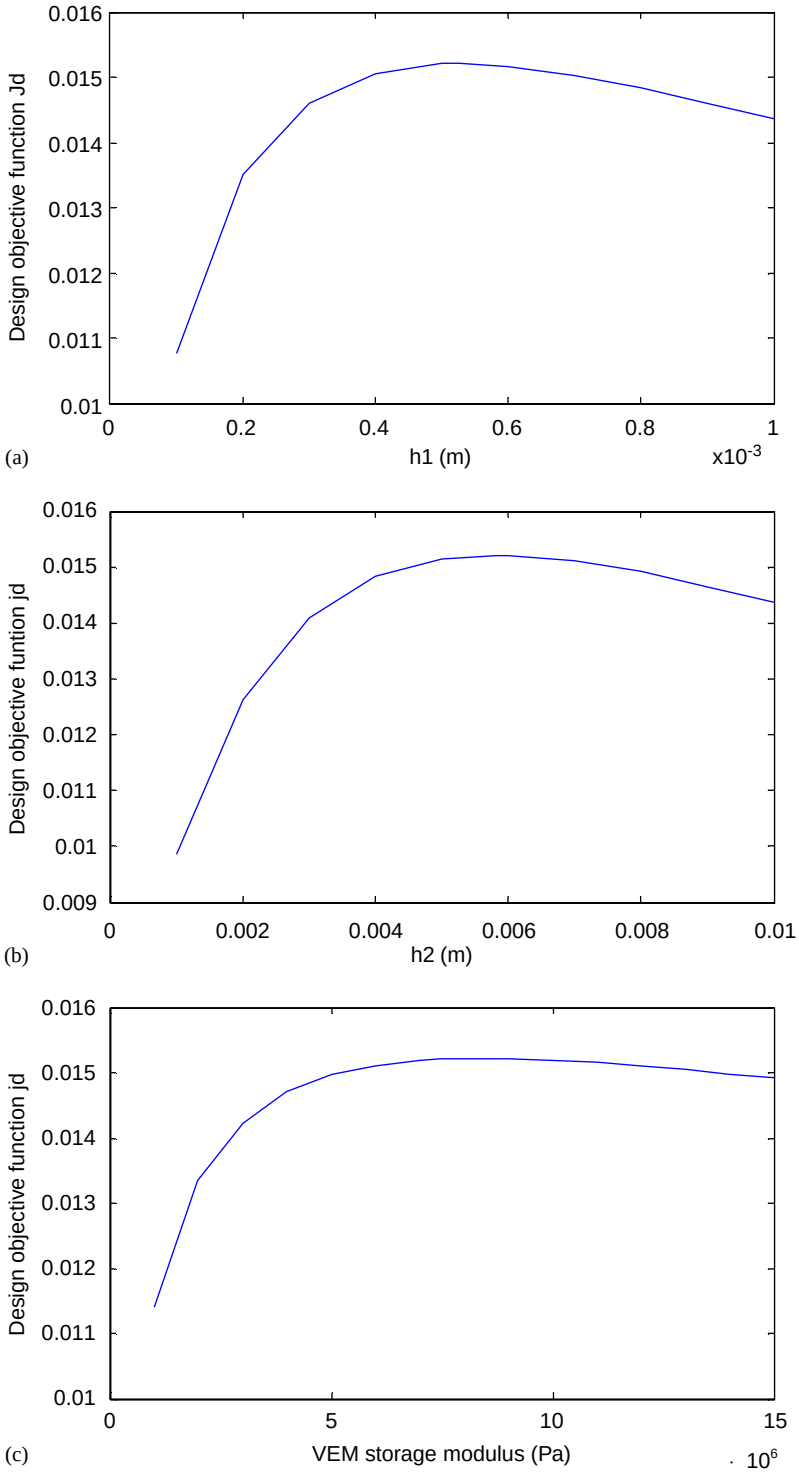

Fig. 3. Design objective function J_d versus different design variables for $\eta = 0.38$ and $\dot{\theta} = 32.9\,\text{rad/s}$: (a) $h_2 = 5.8255\,\text{mm}$, $G_2' = 7.4704\,\text{MPa}$, (b) $h_1 = 0.52562\,\text{mm}$, $G_2' = 7.4704\,\text{MPa}$, and (c) $h_1 = 0.52562\,\text{mm}$, $h_2 = 5.8255\,\text{mm}$.

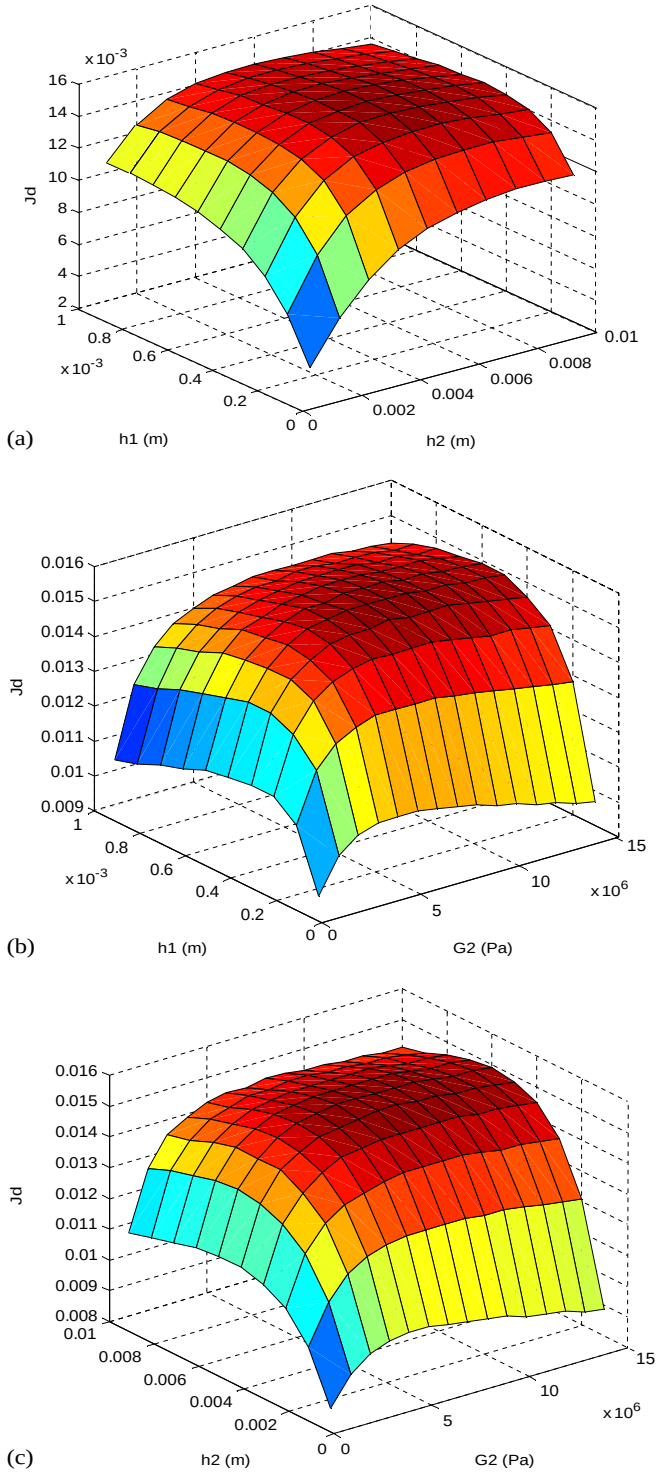

Fig. 4. Effect of different design variables on the design objective function J_d for $\eta = 0.38$ and $\dot{\theta} = 32.9\,\mathrm{rad/s}$: (a) $G_2' = 7.4704\,\mathrm{MPa}$, (b) $h_2 = 5.8255\,\mathrm{mm}$ and (c) $h_1 = 0.52562\,\mathrm{mm}$.

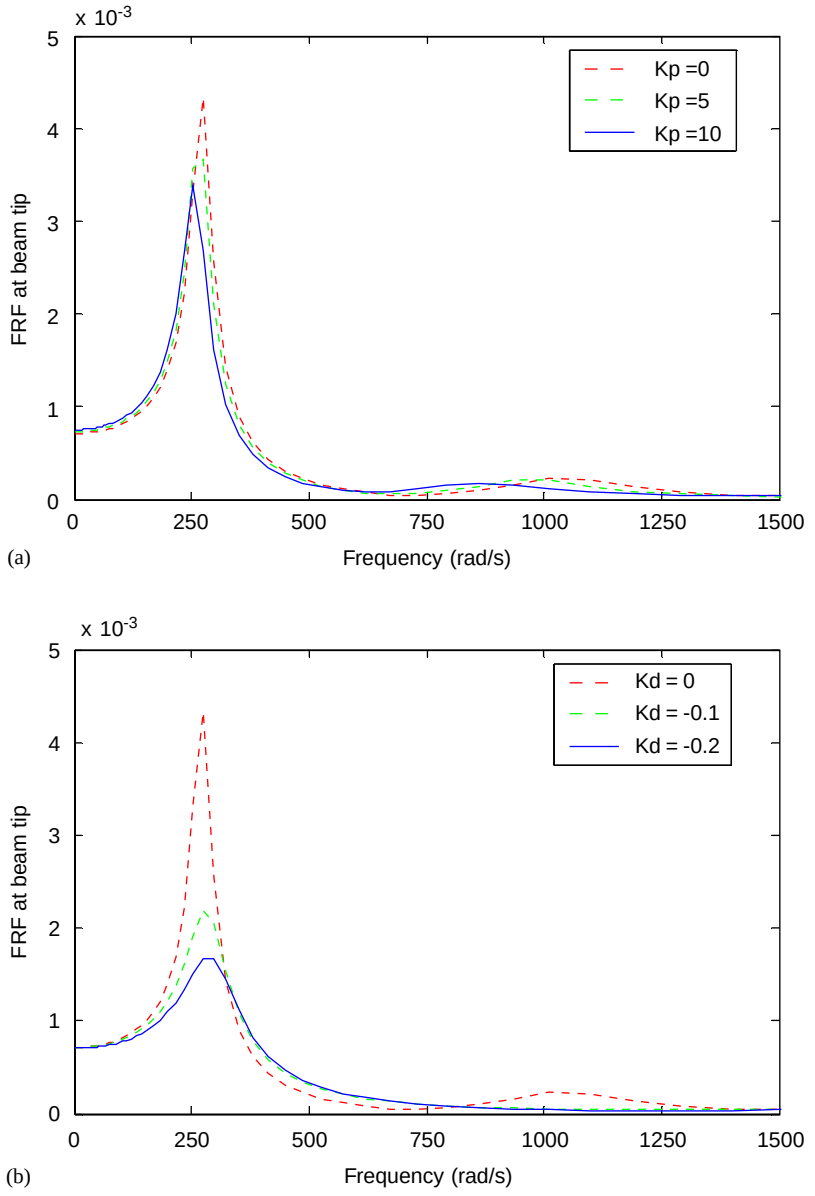

Fig. 5. Frequency response function (FRF) of beam tip using the optimal design variables for $\eta = 0.38$ and $\dot{\theta} = 32.9\,\text{rad/s}$: (a) $K_d = 0$ and (b) $K_p = 0$.

The VEM loss factor η of 0.38 and angular velocity $\dot{\theta}$ of 32.9 rad/s are chosen to perform both the design and control optimization. The design optimization results are

$$h_1 = 0.52562\,\text{mm}, \quad h_2 = 5.8255\,\text{mm}, \quad G_2' = 7.4704\,\text{MPa},$$
$$J_d = 0.01521, \qquad h_2/h_3 = 2.5483$$

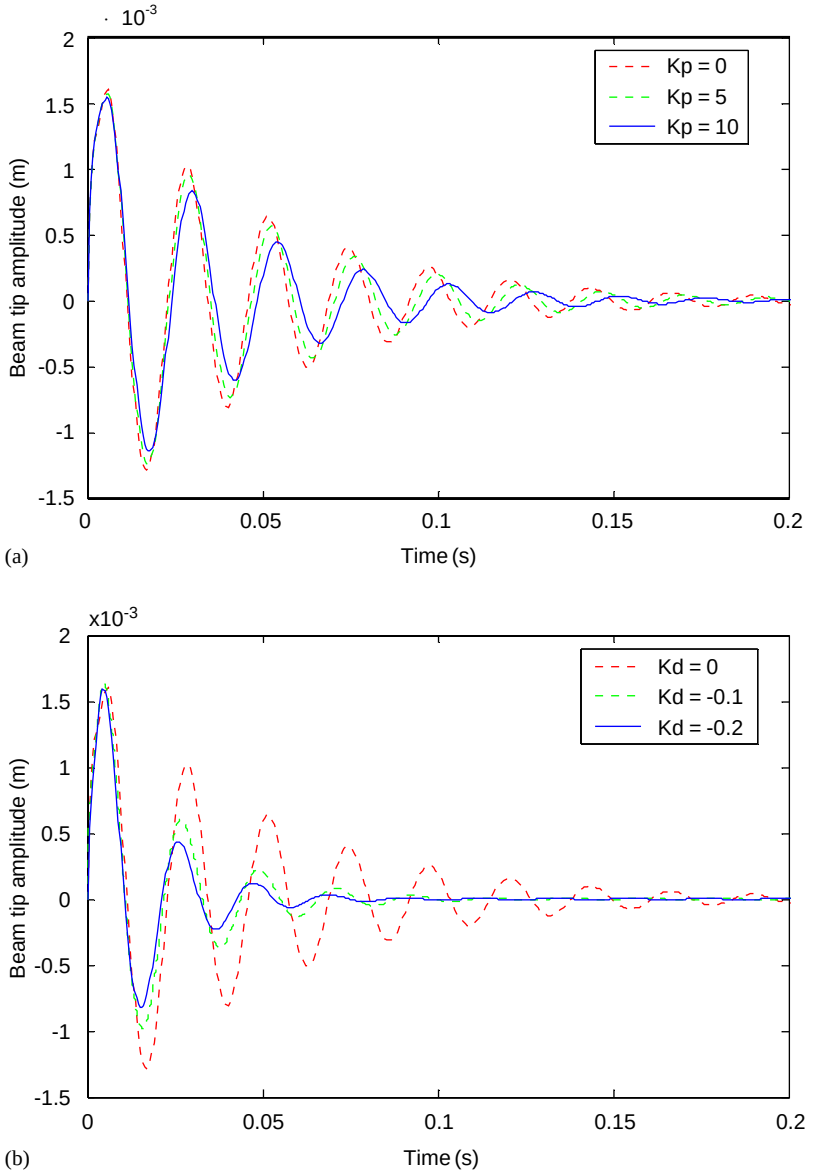

Fig. 6. Impulse response of beam tip using the optimal design variables for $\eta = 0.38$ and $\dot{\theta} = 32.9$ rad/s: (a) $K_d = 0$ and (b) $K_p = 0$.

The effect of h_1, h_2 and G_2' on the design objective function J_d for $\eta = 0.38$ and $\dot{\theta} = 32.9$ rad/s is shown in Figs. 3 and 4. Fig. 3 shows that J_d increases with increase in h_1 and h_2 until the maximum value is reached and then decreases with further increase in h_1 and h_2. These results can be explained as follows. Increasing the thickness h_1 and h_2 will increase the open-loop modal damping ratios for the first three modes considered. However, this occurs at the expense of increasing the weight of the damping treatment. Hence J_d will reach a maximum value at the

optimal values of h_1 and h_2. The effect of G_2' on J_d shows similar result but after the maximum value is reached J_d decreases more slowly with further increase of G_2'. It is shown in Ref. [12] that increasing the beam angular velocity $\dot{\theta}$ will decrease the open-loop modal damping ratios. Hence J_d will decrease with increase of $\dot{\theta}$.

The optimal design variables as determined from the above open-loop design optimization are used in the optimal control problem. The optimal controller gains K_p and K_d are determined by solving the min–max problem (13). The constraint conditions for the control gains are $0 \leqslant K_p \leqslant 10$ and $-0.5 \leqslant K_d \leqslant -0.1$. The weighting matrices $\mathbf{Q}$ and $\mathbf{R}$ in Eq. (11) are selected as identity matrices. The results of the optimal control are $K_p = 0$ and $K_d = -0.2$. Hence the optimal controller is a derivative feedback controller.

Fig. 5 shows frequency response function (FRF) of the beam tip when a unit harmonic point load is applied at the centre of the tip [15]. It can be seen that the tip amplitude is reduced when K_p is more positive or when K_d is more negative. However for stable numerical results, K_p is set to vary in the range $0 \leqslant K_p \leqslant 10$ whereas K_d is set to vary in the range $-0.5 \leqslant K_d \leqslant -0.1$. The results show that the derivative control is more effective in suppressing the tip vibration as compared to the proportional counterpart.

The impulse response of the beam tip for different values of K_p and K_d is shown in Fig. 6. Similar to the findings of Fig. 5, it is evident that the closed-loop response outperforms the open-loop one.

5. Conclusions

This paper has presented optimal design and control of a rotating flexible arm with ACLD treatment. A PD controller is used in the feedback control law. The finite element governing equations of motion of the system are presented. The optimal PZT actuator thickness, viscoelastic layer thickness and storage shear modulus of the VEM core are determined by maximizing a design objective function. The optimal control gains are determined by solving a min–max control problem. Results are also presented for the frequency response and impulse response of the beam tip under different control gains. The results clearly show that the closed-loop response outperforms the open-loop one and also the derivative control is more effective in suppressing the vibration as compared to the proportional counterpart.

Acknowledgements

The authors would like to thank The Hong Kong Polytechnic University for the financial support (Project No. G-YC94) towards this work.

References

[1] A. Baz, J. Ro, Vibration control of rotating beams with active constrained layer damping, *Smart Materials and Structures* 10 (2001) 112–120.

[2] A. Baz, J. Ro, Performance characteristics of active constrained layer damping, *Shock and Vibration* 2 (1995) 33–42.
[3] A. Baz, J. Ro, Optimum design and control of active constrained layer damping, *Journal of Mechanical Design* 117B (1995) 135–144.
[4] A. Baz, Optimization of energy dissipation characteristics of active constrained layer damping, *Smart Materials and Structures* 6 (1997) 360–368.
[5] M.A. Trindade, A. Benjeddou, R. Ohayon, Modeling of frequency-dependent viscoelastic materials for active-passive vibration damping, *Journal of Vibration and Acoustics* 122 (2000) 169–174.
[6] M.A. Trindade, A. Benjeddou, R. Ohayon, Piezoelectric active vibration control of damped sandwich beams, *Journal of Sound and Vibration* 246 (2001) 653–677.
[7] A. Badre-Alam, K.W. Wang, F. Gandhi, Optimization of enhanced active constrained layer (EACL) treatment on helicopter flexbeams for aeromechanical stability augmentation, *Smart Materials and Structures* 8 (1999) 182–196.
[8] Y. Liu, K.W. Wang, Damping optimization by integrating enhanced active constrained layer and active-passive hybrid constrained layer treatments, *Journal of Sound and Vibration* 255 (2002) 763–775.
[9] A. Lumsdaine, Topology optimization of constrained damping layers treatments, *Proceedings of ASME International Mechanical Engineering Congress and Exposition* IMECE2002-39021, 2002.
[10] S. Devasia, T. Meressi, B. Paden, E. Bayo, Piezoelectric actuator design for vibration suppression: placement and sizing, *Journal of Guidance, Control, and Dynamics* 16 (1993) 859–864.
[11] Y.-G. Sung, Modelling and control with piezoactuators for a simply supported beam under a moving mass, *Journal of Sound and Vibration* 250 (2002) 617–626.
[12] E.H.K. Fung, D.T.W. Yau, Vibration characteristics of a rotating flexible arm with ACLD treatment, *Journal of Sound and Vibration* 269 (2004) 165–182.
[13] A.K. Lall, N.T. Asnani, B.C. Nakra, Vibration and damping analysis of rectangular plate with partially covered constrained viscoelastic layer, *Journal of Vibration, Acoustics, Stress, and Reliability in Design* 109 (1987) 241–247.
[14] F.L. Lewis, *Applied Optimal Control and Estimation*, Prentice-Hall, Englewood Cliffs, NJ, 1992.
[15] S.C. Huang, D.J. Inman, E.M. Austin, Some design considerations for active and passive constrained layer damping treatments, *Smart Materials and Structures* 5 (1996) 301–313.